

Manipulation of the vortex motion in nanostructured ferromagnetic/superconductor hybrids

A. V. Silhanek,^{a)} W. Gillijns, and V. V. Moshchalkov

INPAC-Institute for Nanoscale Physics and Chemistry, Nanoscale Superconductivity and Magnetism and Pulsed Fields Group, Katholieke Universiteit Leuven, Celestijnenlaan 200 D, B-3001 Leuven, Belgium

V. Metlushko and F. Gozzini

Department of Electrical and Computer Engineering, University of Illinois, Chicago, Illinois 60607

B. Ilic

Cornell Nanofabrication Facility, School of Applied and Engineering Physics, Cornell University, Ithaca, New York 14853

W. C. Uhlig and J. Unguris

National Institute of Standards and Technology, 100 Bureau Drive Stop 8412 Gaithersburg, Maryland 20899-8412

(Received 16 February 2007; accepted 22 March 2007; published online 30 April 2007)

The authors investigate the rectified motion of vortices in superconducting films deposited on top of a close-packed array of open in-plane magnetized triangular micromagnets. The dc voltage induced by the vortex drift under an ac excitation is recorded for three different magnetic configurations of the triangles. When the magnetic elements are in the as-grown state a rectification signal which reverses sign when the field changes polarity is observed. In contrast to that, when the array of triangles is magnetized the observed rectification effect is independent of the field polarity and can be reverted by reorienting the magnetization of the micromagnets. © 2007 American Institute of Physics. [DOI: 10.1063/1.2734874]

During the last years intense research efforts have been focused on study and control of the vortex motion in superconducting materials. Special attention has been paid to the ratchet motion induced by asymmetric pinning potentials.^{1,2} This effect manifests itself as a net vortex motion arising along a specific direction when the system is exposed to a deterministic zero-average ac excitation. The basic condition for the ratchet effect is the presence of a pinning landscape lacking inversion symmetry in scales of the order of the superconducting coherence lengths ξ and the penetration depth λ . Interestingly, by properly designing the underlying pinning structure it is possible to use the resulting rectification effect to either clear or concentrate magnetic flux quanta in fluxonics devices.³

A convincing evidence for this kind of vortex ratchet motion has been found in systems with triangular magnetic dots¹ and for two interpenetrating square lattices of big and small square holes.² In either case the predefined asymmetric shape of the pinning center give rise to a vortex drift which is field polarity independent and is limited to a very specific direction with no freedom to reverse it. Recently Carneiro⁴ proposed an alternative ratchet effect that can be realized by using an array of in-plane magnetized dots.⁵ In contrast to the standard (nonmagnetic) ratchet motion, this dipole-induced motion can be switched by varying the orientation of the local magnetic moments thus paving the way towards full control of the direction of the average vortex displacement.

In this work we explore the vortex rectification effects induced by an array of magnetic triangular rings lying underneath a superconducting material. The used magnetic and

superconducting materials involve substantially different scale of energies (i.e., upper critical field of the superconductor is much smaller than the coercive field of the magnets) thus allowing us to investigate the superconducting phase without perturbing the magnetic state of the rings. Transport measurements reveal that different sort of ratchet motions take place depending on the magnetic state of the rings. In particular, we show that the net direction of the vortex motion can be reversed by simply changing the magnetic state of the triangles. These observations are in agreement with recent theoretical predictions by Carneiro.⁴

The used sample consists of a closely packed triangular array of Permalloy (Py) equilateral triangular loops (250 nm wide, 23 nm thick, with lateral size $d=2\ \mu\text{m}$ and apart $s=250\ \text{nm}$) fabricated by electron-beam lithography and subsequent lift-off techniques. A 5 nm thick Si layer separates the magnetic template from the superconducting film in such a way that the interaction between them is mainly magnetic.⁶ The superconducting Al film (thickness of 50 nm) is evaporated in a molecular-beam epitaxy apparatus at a rate of 1.7 nm/min at room temperature. In order to ensure a homogeneous current distribution the Al films are evaporated onto a predefined photoresist mask patterned into a transport bridge aligned along the x axis [see Fig. 1(a)]. For a direct comparison, in all cases patterned and unpatterned Al film are coevaporated. The average roughness of the plain films is about 5 nm and exhibits a residual resistivity ratio of ~ 2 . From the superconductor/normal phase boundary, as determined by 10% normal state resistance criterion [see solid square symbols in Fig. 3(a)], a superconducting coherence length $\xi \sim 120\ \text{nm}$ at zero temperature is estimated.

It has been recently shown that a multiply connected magnetic triangle can be set in eight different magnetic

^{a)}Electronic mail: alejandro.silhanek@fys.kuleuven.be

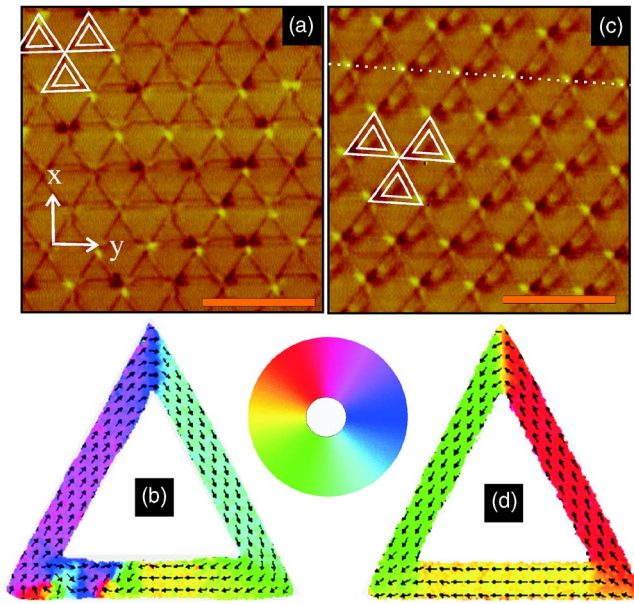


FIG. 1. (Color online) Magnetic force microscopy images of a triangular array of magnetic triangular loops (a) in the as-grown state and (c) in the magnetized state. The white triangles emphasize the close-packed triangular array. The bottom right bars indicate $5 \mu\text{m}$ scale. In-plane magnetization of individual elements obtained by scanning electron microscopy with polarized analysis for an (b) as-grown state and (d) magnetized state. The color code shown in the disk indicates the orientation of the in-plane magnetization.

states, namely, two flux-closure states of opposite chirality and two magnetized states of opposite polarization for each side of the triangle.⁷ Most of the spectrum of possible states can be indeed observed in the magnetic force microscopy (MFM) image shown in Fig. 1(a) for the patterned sample in the as-grown state. In this figure the bright(dark) spots at the vertices of the triangles indicate a positive(negative) z component of the stray field (B_z) generated by the rings when they are in the magnetized state.⁸ In contrast to that, the flux-closure state can be identified by a much weaker out-of-plane stray field ($B_z \sim 0$). One of the most obvious features of Fig. 1(a) is the lack of order in the distribution of bright and dark spots. In some cases two dark (or bright) spots can be found in close proximity thus suggesting that there is little interaction between neighboring elements. A detailed scanning electron microscopy with polarized analysis⁹ (SEMPA) image of the in-plane magnetization distribution in one of the magnetic elements [see Fig. 1(b)] shows a richer structure than that revealed by the MFM analysis. In this case an open triangle in an almost flux-closure state exhibits two small magnetic vortices along the base of the triangle. The color code for the in-plane magnetic orientation is shown by the colored disk in Fig. 1.

A different situation emerges when the triangles are magnetized by applying an in-plane magnetic field $H = 800$ mT along the $+y$ direction. The resulting MFM image corresponding to the remanent state ($H=0$) is shown in Fig. 1(c). In this case a highly ordered structure of staggered magnetic stray field can be observed. As shown by the SEMPA image in Fig. 1(d) in this case the disorder is not only removed at large scales but also at scales of single elements where now every side of the triangles is in a single domain state.

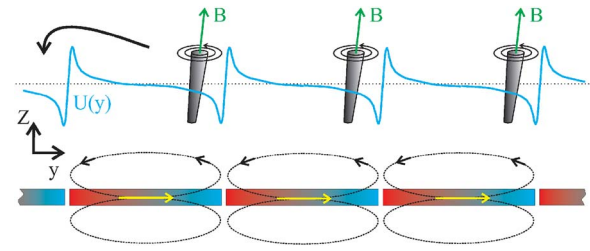


FIG. 2. (Color online) Schematic presentation of a cross section along the white dotted line shown in Fig. 1(c) after the rings were magnetized with $H \parallel +y$. The stray field originated in the dipoles is indicated as dashed lines. The resulting pinning potential $U(y)$ and the net flux motion for an ac-current excitation along x are shown in the upper part of the drawing.

Interestingly when the microloops are set in the magnetized state they form a triangular array of in-plane dipoles [pairs of dark and bright spots in Fig. 1(c)] with equal periodicity than the array of triangles. This situation is schematically illustrated in Fig. 2 with a cross section of the pattern along the dotted white line shown in Fig. 1(c). In this picture the magnetic triangles yield an out-of-plane component which progressively switches from negative, at the far left side of one ring, to positive on the extreme right corner. When placed in a row these magnets generate a stray field with B_z following an asymmetric spatial modulation. The interaction between this field component and the flux lines produces a minimum in the pinning potential where B_z maximizes, as shown with a solid line in Fig. 2. This potential $U(y)$ mirrors the shape of the B_z profile inverting the asymmetry and hence producing an also asymmetric pinning force $F = -\partial_y U$. Under these circumstances, if the system is submitted to an oscillatory drive along x with zero average, a net motion of the flux line lattice will be induced towards $-y$. This is indeed confirmed by the dc output voltage V_{dc} recorded under a sinusoidal ac current I_{ac} , as shown in Fig. 3, for different scenarios.

For a completely symmetric pinning landscape like the one provided by a plain film, V_{dc} is expected to be negligible. However, Fig. 3(a) shows that in our unpatterned samples a clear $V_{dc} \neq 0$ appears. This result can be attributed, for ex-

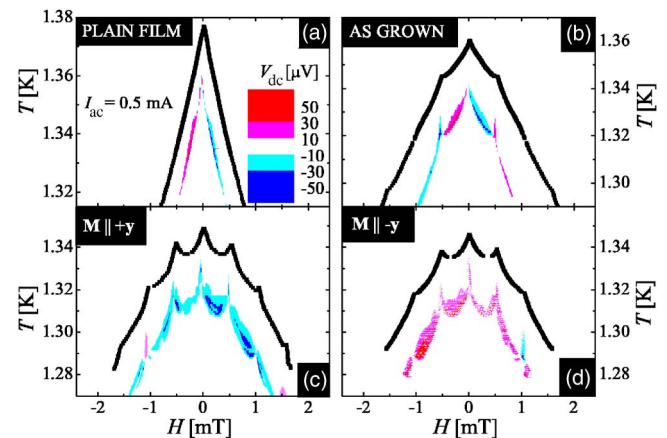


FIG. 3. (Color online) Rectified voltage V_{dc} as a function of field and temperature for a sinusoidal excitation of amplitude $I_{ac} = 1$ mA and frequency of 1 kHz for (a) plain film with no patterning underneath, (b) triangular micromagnets in the as-grown state, (c) triangular magnets magnetized along $+y$ and (d) triangular micromagnets magnetized along $-y$. With solid square symbols is indicated the superconductor/normal transition as determined by 10% normal state resistance criterion with $10 \mu\text{A}$.

ample, to inevitable asymmetries between the edge barriers for vortex penetration.^{10,11} For the patterned sample with the triangles in a disordered state [see Fig. 3(b)] two important differences can be distinguished with respect to the plain film. Firstly, commensurability effects consistent with the periodicity of the underlying pinning landscape become apparent.⁸ Secondly, there is a sign reversal of the rectification effect at the first matching field as a result of the vortex-vortex interaction.² It is worth noticing that for both the plain film and the as-grown sample, V_{dc} is an antisymmetric function of field thus indicating that a nonmagnetic ratchet potential dominates the effective vortex motion. It is precisely the unperturbable nature of this standard ratchet motion which allows us to unambiguously separate the contribution coming from the dipole-induced ratchet motion. Indeed, a nonmagnetic pinning landscape is insensitive to the field polarity and so is the vortex drift velocity v_d . Since the measured voltage $V_{dc} \propto v_d H$, positive and negative fields give rise to an opposite sign on V_{dc} .

Let us now consider the dc response shown in Fig. 3(c) corresponding to the case illustrated in Fig. 2 of triangles magnetized along $+y$. Since for $H > 0$ vortices sit in a different position than for $H < 0$, v_d turns out to be an antisymmetric function of H and therefore positive and negative fields give rise to the same signs on V_{dc} . In other words, *vortices and antivortices have an opposite easy motion direction*. Thus, a fingerprint of the dipole-induced ratchet effect is the presence of mirrorlike $V_{dc}(H)$ regions, as indeed observed in Figs. 3(c) and 3(d). Still the most compelling evidence of this type of ratchet potential comes from a direct comparison between the two magnetized configuration shown in Figs. 3(c) and 3(d) as it becomes clear that changing the magnetic state of the dipoles from $-y$ to $+y$ induces a sign change on V_{dc} . This magnetic-history dependent ratchet effect cannot be attributed but to the magnetic state of the underlying array of micromagnets.

To summarize, we have explored the vortex ratchet dynamics of a conventional superconductor on top of a periodic array of micromagnets. The used triangular shape of the

magnets gave us the possibility to easily switch between two opposite magnetized dipolar states. A clear contrast in the rectification properties between the polarized states and the as-grown sample is observed. Essentially the polarized states exhibit a different type of ratchet motion, which is independent of the field polarity and can be selectively switched to control the direction of the net vortex drift. A possible application combining both characteristics is a *switchable vortex lens* consisting of two striped ratchet structures, as those described in Ref. 3, each of which having an oppositely magnetized dipole array (this can be achieved by changing the coercive field of each stripe). Interestingly, this magnetic lens can be switched from concave to convex by simply inverting the dipole orientation with an external in-plane field.

This work was supported by the K.U. Leuven Research Fund No. GOA/2004/02, FWO programs, and by the U.S. NSF, Grant No. ECS-0202780 (VM). One of the authors (A.V.S.) is grateful for the support from the FWO-Vlaanderen.

¹J. E. Villegas, S. Savel'ev, F. Nori, E. M. Gonzalez, J. V. Anguita, R. Garcia, and J. L. Vicent, *Science* **302**, 1188 (2003).

²C. C. de Souza Silva, J. V. de Vondel, M. Morelle, and V. V. Moshchalkov, *Nature (London)* **440**, 651 (2006).

³B. Y. Zhu, F. Marchesoni, and F. Nori, *Physica E (Amsterdam)* **18**, 318 (2003); *Phys. Rev. Lett.* **92**, 180602 (2004).

⁴G. Carneiro, *Phys. Rev. B* **72**, 144514 (2005); *Physica C* **432**, 206 (2005).

⁵C. C. de Souza Silva, A. V. Silhanek, J. van de Vondel, W. Gillijns, V. Metlushko, B. Ilic, and V. V. Moshchalkov, *Phys. Rev. Lett.* **98**, 117005 (2007).

⁶The small change observed in the superconducting critical temperature between the patterned and unpatterned samples ensures an effective suppression of proximity effects.

⁷A. Imre, E. Varga, L. L. Ji, B. Ilic, V. Metlushko, G. Csaba, A. Orlov, G. H. Bernstein, and W. Porod, *IEEE Trans. Magn.* **42**, 3641 (2006).

⁸A. V. Silhanek, W. Gillijns, V. V. Moshchalkov, V. Metlushko, and B. Ilic, *Appl. Phys. Lett.* **89**, 182505 (2006).

⁹M. R. Scheinfein, J. Unguris, M. H. Kelley, D. T. Pierce, and R. J. Celotta, *Rev. Sci. Instrum.* **61**, 2501 (1990).

¹⁰D. Y. Vodolazov and F. M. Peeters, *Phys. Rev. B* **72**, 172508 (2005).

¹¹V. V. Pryadun, J. Sierra, F. G. Aliev, D. S. Golubovic, and V. V. Moshchalkov, *Appl. Phys. Lett.* **88**, 062517 (2006).